A TEM study on the microstructure of rapidly solidified Cu–Y alloys

X. ZHANG, A. ATRENS
Department of Mining and Metallurgical Engineering, The University of Queensland, Queensland, Australia 4072

The microstructure of rapidly solidified copper–yttrium alloys was studied by TEM. For the near-eutectic alloys, the following observations were made: melt-spun Cu–12.5 wt % Y whiskers showed a very fine eutectic of f.c.c. copper and hexagonal Cu_5Y plus isolated areas of a new metastable orthorhombic phase, Cu_9Y; melt-spun Cu–51.1 wt % Y whiskers contained an amorphous matrix plus precipitates of the equilibrium phase orthorhombic Cu_2Y. For far-from-eutectic alloys, glass formation was detected in the melt-spun whiskers of Cu–25.0 wt % Y alloy, while the melt-spun Cu–18.9 wt % Y whiskers showed a fine-grained single phase Cu_5Y, an easily formed metastable phase, and melt-spun Cu–41.6 wt % Y showed an ultrafine single phase Cu_2Y, an equilibrium orthorhombic phase.

1. Introduction
Glass formation has been reported for eutectic alloys by melt spinning [1, 2] and by sputtering [3, 4] in the Cu–Y system, whilst the microstructure of rapidly solidified alloys with compositions far from eutectic has not yet been investigated. The present paper reports a TEM investigation on the microstructure of rapidly solidified intermetallic alloys and some eutectic alloys in the Cu–Y system.

2. Experimental procedure
Cu–Y alloys with compositions listed in Table I were produced by melting high-purity copper (99.99%) and yttrium (99.9%) under a very low pressure of argon in a Leybold–Heraeus induction vacuum furnace. After the metals were melted, high-purity argon was let into the chamber through a getter of pure copper scraps heated to about 500 °C by a separate resistance tube furnace until a positive pressure was reached. Then strong stirring was applied to the melt by an alumina rod inserted into the alumina crucible.

Melt spinning was performed in a low-pressure atmosphere of argon in a horizontal inner peripheral melt spinner [5]. The alloy charge was heated to about 100–200 °C above the corresponding liquidus temperature in an alumina nozzle crucible by high-frequency induction heating and jetted by an argon pressure of about 20–30 psi (140–210 kPa) on to the inner periphery of a pure copper wheel running at a tangential speed of about 22 m s^{-1}. Ribbons of thickness 30–60 μm were produced. By carefully controlling the jetting pressure, whiskers with thickness ranging from 3 to 10 μm were also produced. This paper focuses on these whiskers. Assuming a heat transfer coefficient of around 5×10^5 W m^{-2} K^{-1} which is appropriate for a wheel speed of 22 m s^{-1}, the

calculated cooling rates around the liquidus temperature using a one-dimensional heat transfer model [6], taking into account the temperature increase of the substrate with estimated thermophysical properties, are 3.1×10^7 °C s^{-1} for 3 μm thick whiskers and 7.3×10^6 °C s^{-1} for 10 μm thick whiskers.

3. Results
3.1. Rapidly solidified Cu–12.5 wt % Y
Fig. 1a is a TEM bright-field micrograph of the eutectic matrix taken on a Jeol 4000 FX AEM (400 kV). Fig. 1b is a diffraction pattern taken from the eutectic matrix shown in Fig. 1a. It was indexed as a combined ring pattern of f.c.c. copper and hexagonal Cu_5Y. The d values and intensity of the major rings in the pattern agree well with those predicted (Table II). Cu_5Y is a metastable phase which is easily formed by rapid solidification of copper–yttrium alloys of compositions in this neighbourhood.

Apart from the eutectic matrix, isolated areas of a few grains with grain size in the range from 0.2 to 0.6 μm were also observed in melt-spun Cu–12.5 wt % Y whiskers. Fig. 2 shows such an area. Electron diffraction [7] showed that they were of the same

TABLE I Compositions of Cu–Y alloys studied

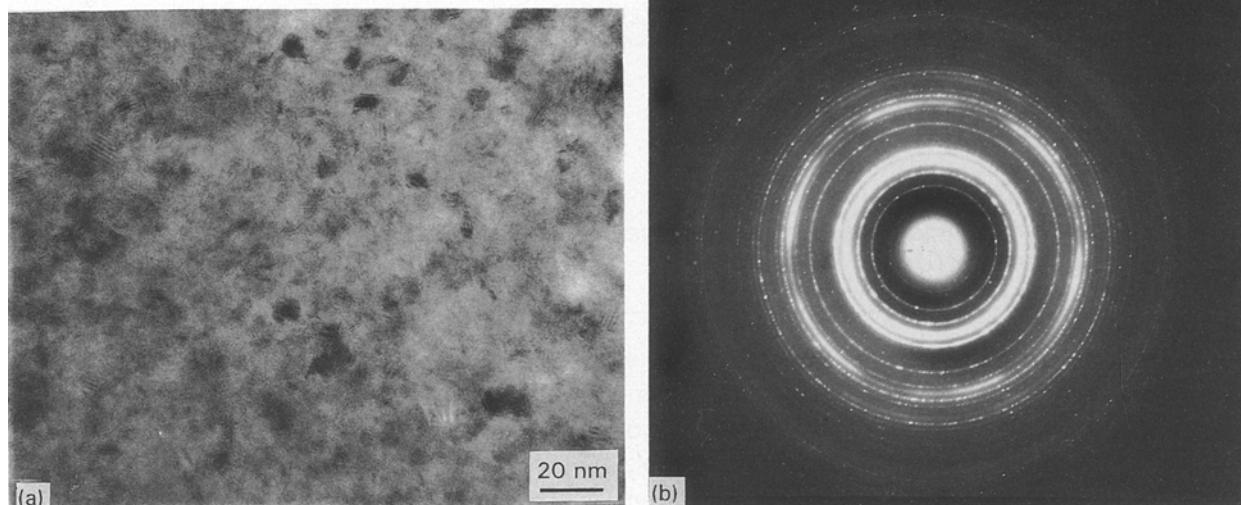| Alloy	Analysed composition (wt %)	
	Cu	Y
Cu–12.5 wt % Y	87.4	12.5
Cu–18.9 wt % Y	82.1	18.9
Cu–25.0 wt % Y	75.0	25.0
Cu–41.6 wt % Y	58.4	41.6
Cu–51.1 wt % Y	48.9	51.1

Figure 1 (a) TEM bright-field micrograph of ultrafine eutectic matrix taken from a Cu–12.5 wt % Y alloy whiskers; (b) selected-area diffraction pattern from the area shown in (a).

TABLE II Comparison of d values and intensities with identified phases for the ring pattern in Fig. 1b

Pattern		f.c.c. Cu			Cu_5Y		
d (nm)	Intensity[a]	$(h k l)$	d (nm)	Intensity	$(h k l)$	d (nm)	Intensity
0.2433	3rd				(1 1 0)	0.2488	3rd
0.2083	1st	(1 1 1)	0.2088	1st	(1 1 1)	0.2129	1st
					(0 0 2)	0.2051	3rd
0.1866	2nd	(2 0 0)	0.1808	2nd	(2 0 1)	0.1910	3rd
0.1263	4th	(2 2 0)	0.1278	3rd	(2 2 0)	0.1248	2nd
0.1199	5th				(1 1 3)	0.12016	1st

[a] 1st = strongest, etc.

phase. The phase was identified [7] as a metastable orthorhombic phase Cu_9Y (not previously identified) which is pseudo-hexagonal and pseudo-tetragonal.

3.2. Rapidly solidified Cu–18.9 wt% Y

Fig. 3a is a TEM bright-field micrograph taken from a specimen of Cu–18.9 wt % Y whiskers on a Hitachi H-800 STEM (200 kV). It shows an area of several grains with grain size in the range of 0.2 to 0.4 μm. Fig. 3b, c and d are convergent-beam microdiffraction patterns with a very small spot size and a very small beam convergence angle (α_s), taken from inside some of the grains shown in Fig. 3a. They all can be indexed as Cu_5Y patterns with different zone axes, as shown by the indexing beside each diffraction pattern. Therefore the grains shown in Fig. 3a are all of the same phase, hexagonal Cu_5Y (space group P_6/mmm).

3.3. Rapidly solidified Cu–25.0 wt% Y

Fig. 4a is a TEM bright-field micrograph taken from Cu–25.0 wt % Y whiskers on a Jeol 4000 FX AEM at 400 kV. Fig. 4b shows a selected-area diffraction pattern from the area shown in Fig. 4a. This ring pattern can be indexed as a combined pattern of equilibrium phases, hexagonal Cu_4Y and orthorhombic Cu_2Y.
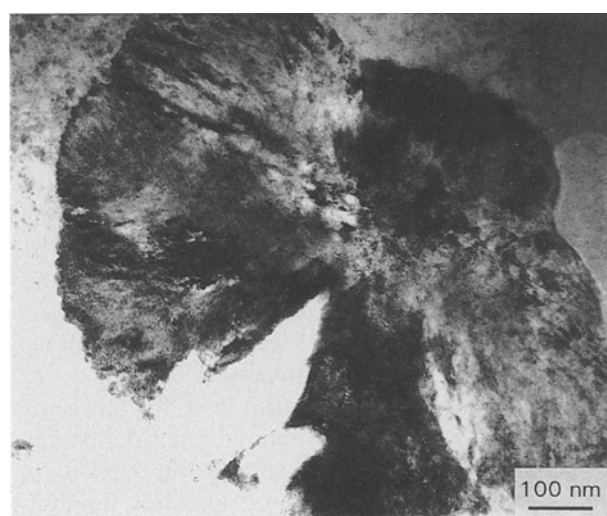

Figure 2 TEM micrograph showing an isolated area of the metastable Cu_9Y phase consisting of several grains surrounded by eutectic matrix (taken on Jeol 4000 FX AEM at 400 kV).

The d values and intensities of the major rings are compared with data for these phases in Table III. The agreement is very good. Judging from the extensive diffuse scattering, the presence of glass was also likely. This was further supported by the extensive diffuse
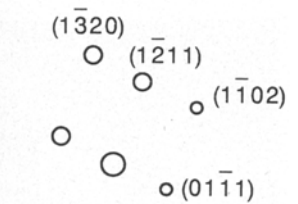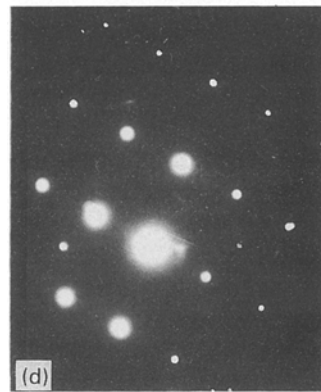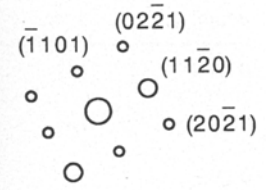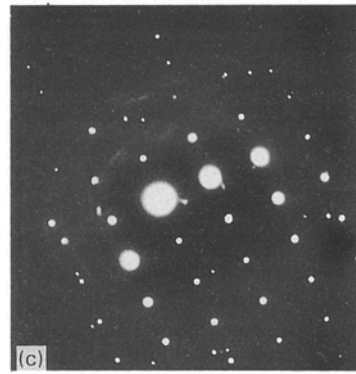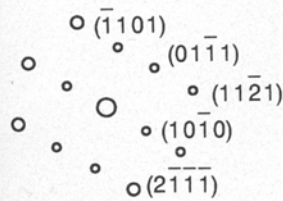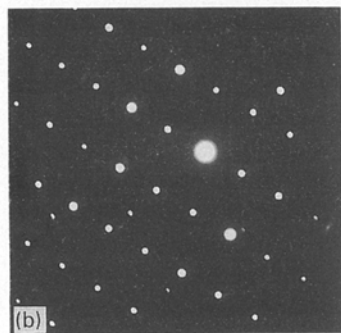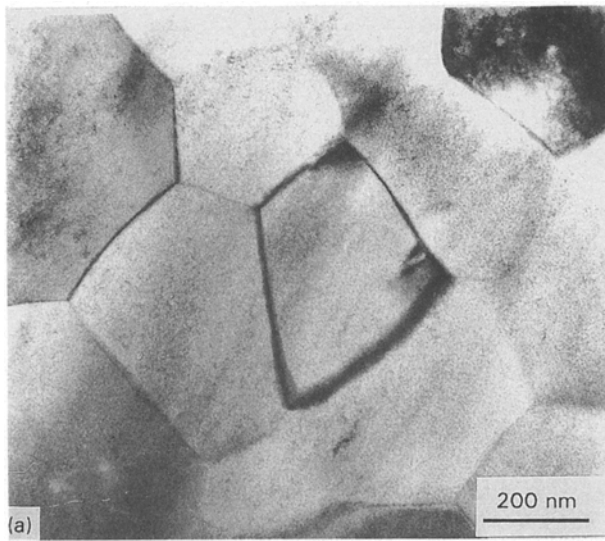
Figure 3 (a) TEM bright-field micrograph taken from the Cu–18.9 wt % Y alloy whisker, showing grains of single-phase Cu_5Y. (b–d) Convergent-beam micro-diffraction patterns taken from inside the grains shown in (a); the indexings are shown beside each pattern. $Z = [1\bar{2}13]$ for (b), $[1\bar{1}02]$ for (c), $[\bar{5}143]$ for (d).
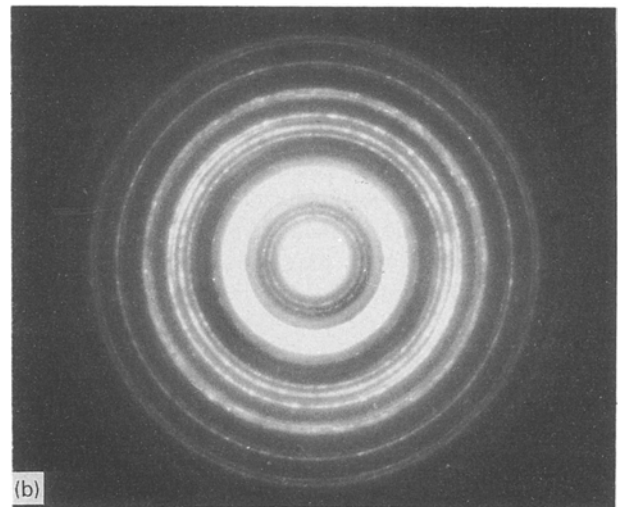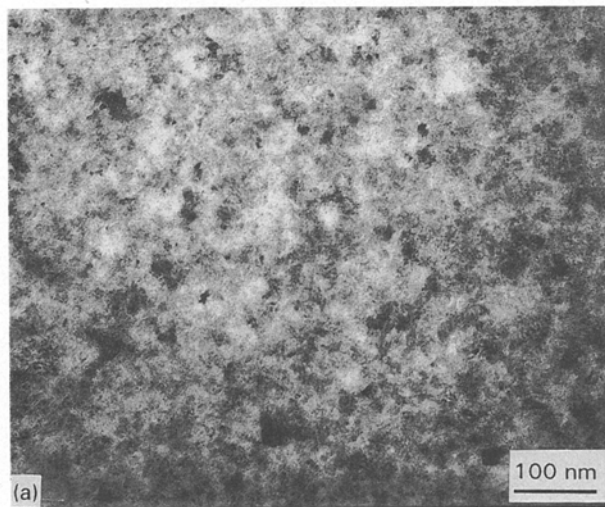

Figure 4 (a) TEM bright-field micrograph taken from Cu–25.0 wt % Y whisker; (b) selected-area diffraction pattern taken from the area shown in (a) showing a mixture of Cu_4Y and Cu_2Y phases.

scattering in a convergent-beam microdiffraction pattern from an area of about 0.1 μm diameter, taken from the edge of a hole in the specimen.

3.4. Rapidly solidified Cu–41.6 wt% Y

Fig. 5a is a TEM bright-field micrograph taken from Cu–41.6 wt % Y whiskers on the Jeol 4000 FX AEM

(at 400 kV). It shows an ultrafine grain structure. The grain size is in the range from 10 to 50 nm. Fig. 5b is a selected-area diffraction pattern taken from an area in Fig. 5a. The pattern has rings with diameters which correspond to the d spacings of some planes of the equilibrium orthorhombic phase Cu_2Y, but the intensity distribution among the rings is quite different from the intensity distribution for this phase as shown

TABLE III Comparison of d values and intensities with identified phases for the ring pattern in Fig. 4c

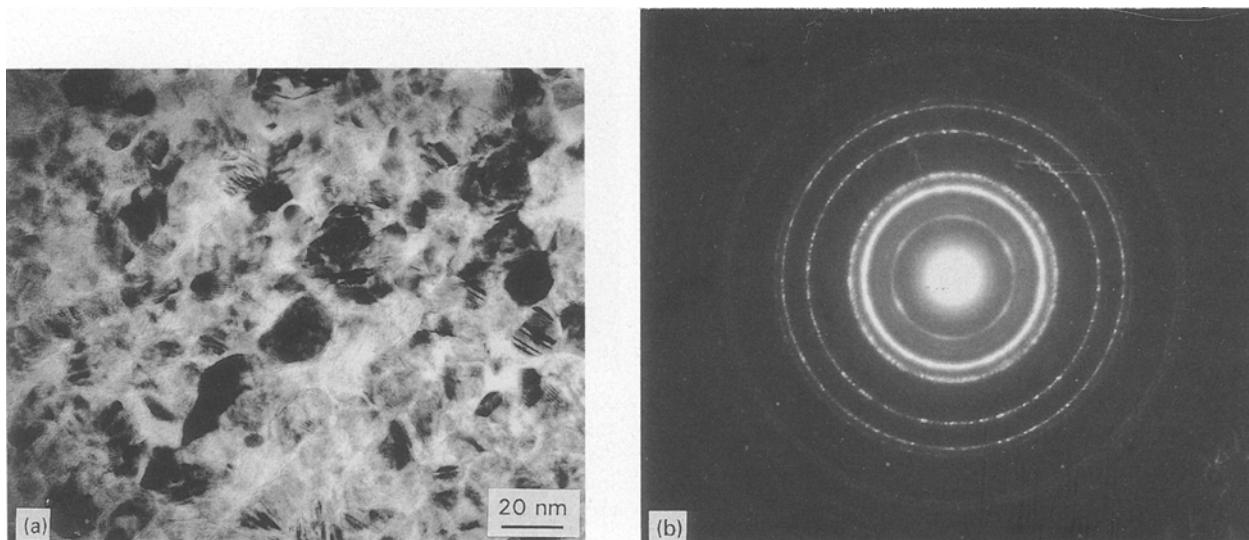| Pattern		Cu$_4$Y			Cu$_2$Y		
d (nm)	Intensity	$(h\,k\,l)$	d' (nm)	Intensity	$(h\,k\,l)$	d (nm)	Intensity
0.2415	2nd	(1 1 0)	0.2470	2nd	(1 1 2)	0.2558	2nd
					(0 2 2)	0.2493	1st
0.2101	1st	(1 1 2)	0.2120	1st	(1 0 3)	0.2103	1st
		(2 0 0)	0.2137	3rd	(2 0 0)	0.2136	2nd
0.1323	3rd	(3 0 2)	0.1351	2nd	(1 3 4)	0.1350	2nd
0.1256	5th	(2 2 0)	0.1240	3rd	(2 4 2)	0.1257	5th
0.1217	4th	(1 1 6)	0.1203	3rd	(0 3 5)	0.1231	2nd

Figure 5 (a) TEM bright-field micrograph taken from Cu–41.6 wt % Y whiskers, (b) selected-area diffraction pattern taken from a small area in (a).

in Table IV . There are two possibilities. The first is that the pattern may be from the Cu$_2$Y phase, but the grains have certain orientation in the small areas selected. Note the slightly localized intensity for some of the rings in the pattern. Alternatively, they may be from metastable phases which have similar d spacings as the equilibrium Cu$_2$Y phase. Further study is required to clarify this.

3.5. Rapidly solidified Cu–51.1 wt% Y
Fig. 6a and b are TEM bright-field micrographs taken from the Cu–51.1 wt % Y whiskers on a Hitachi H-800 STEM (200 kV) with different magnifications. Fig. 6c is a convergent-beam microdiffraction pattern taken from an area (spot size $\simeq$ 0.5 μm diameter) in Fig. 6a with a very small beam convergence angle (α_s). It revealed extensive diffuse scattering from the matrix and some spots from the precipitates in the matrix (see Fig. 6a and b). The diffuse scattering from such a small area (0.5 μm diameter) is so strong that it forms haloes and rings instead of the separate small discs expected from crystalline phases. The matrix must therefore be amorphous.

Fig. 6d is a selected-area diffraction pattern taken from one of the precipitates and the surrounding glass matrix on a Jeol 4000 FX AEM. Because of the very

fine size of the precipitates, it is difficult to tilt it without losing sight of the selected precipitate. Thus the pattern was not taken exactly at the zone axis. This rectangular pattern can be indexed as a $[2\,\bar{4}\,\bar{1}\,\bar{1}]$ zone-axis pattern of the equilibrium phase Cu$_2$Y. The indexing is shown beside the pattern in Fig. 6(d). Therefore the precipitates are likely to be Cu$_2$Y phase.

4. Discussion
While high glass formability has been reported [8–10] for some of the intermetallic alloys in the Cu–Ti and Cu–Zr systems, it is quite difficult to form a glass for the intermetallic alloys studied above by melt-spinning in the Cu–Y system. However, easy glass formation was experienced for alloys which undergo phase separation during equilibrium or metastable solidification, for example the Cu–51.1 wt % Y and Cu–25.0 wt % Y alloys. Therefore phase separation which occurs by diffusion, for which activation is necessary, is an important factor affecting glass formation.

During equilibrium solidification, the Cu–25.0 wt % Y alloy solidifies as a single hexagonal Cu$_4$Y phase. The above study showed that it solidified as a mixture of hexagonal Cu$_4$Y and orthorhombic Cu$_2$Y phases

TABLE IV Comparison of d values and intensities with equilibrium phases for the ring pattern in Fig. 5b

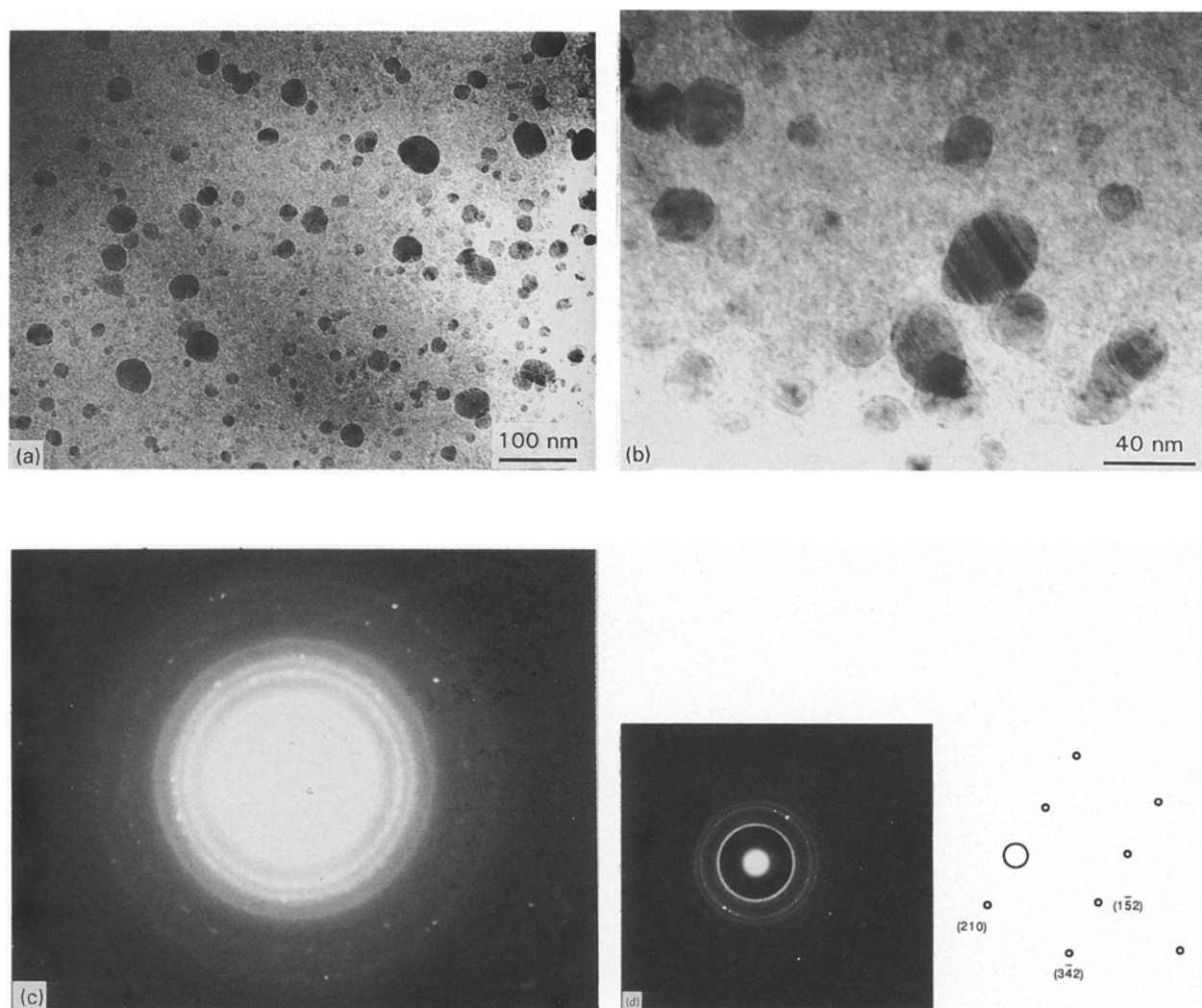| Pattern		Cu$_2$Y			Cu$_4$Y		
d (nm)	Intensity	$(h\,k\,l)$	d (nm)	Intensity	$(h\,k\,l)$	d (nm)	Intensity
					100	0.4261	4th
0.3012	4th		0.304	4th	102	0.2955	2nd
0.2632		112	0.2558	2nd			
0.2404		022	0.2493	1st	110	0.2470	2nd
0.2066	1st	103	0.2103	1st	004	0.2060	4th
0.1786	2nd	211	0.1983	6th	104	0.1860	4th
0.1587		213	0.1563	3rd	114	0.1586	3rd
0.1253	3rd	035	0.1231	2nd	220	0.1240	3rd

Figure 6 (a, b) TEM bright-field micrographs taken from the Cu–51.5 wt % Y whiskers, showing the amorphous matrix with precipitates. (c) Convergent-beam microdiffraction pattern with small beam convergence angle taken from a small area in (a); the extensive diffuse scattering suggests the amorphous nature of the matrix. (d) Selected-area diffraction pattern taken from a small area including a precipitate and the surrounding in (b); $Z = [2\,\bar{4}\,\bar{1}\,\bar{1}]$.

plus glass in melt spinning. This suggests that the phase boundary in the equilibrium phase diagram may have been changed in this composition neighbourhood by rapid solidification. The phase separation in melt spinning may have caused the glass formation which was detected in the Cu–25.0 wt % Y whiskers.

On the other hand, the high glass formability of congruent intermetallic alloys in the Cu–Ti and Cu–Zr systems reported [8–10] suggested that the crystallization of such congruent intermetallic alloys also require activation, though no phase separation is involved.

5. Conclusions

1. Melt-spun Cu–12.5 wt % Y alloy whiskers showed a fine eutectic of f.c.c. copper and hexagonal Cu$_5$Y plus isolated areas of a new metastable orthorhombic phase, Cu$_9$Y.

2. Melt-spun Cu–18.9 wt % Y alloy whiskers contained fine grains of a single phase, the metastable Cu$_5$Y phase with a hexagonal structure.

3. Melt-spun Cu–25.0 wt % Y whiskers consisted of a mixture of the hexagonal Cu_4Y and orthorhombic Cu_2Y phases. Glass was also detected in whiskers of this far-from-eutectic alloy.

4. Melt-spun Cu–41.6 wt % Y whiskers showed an ultrafine grain structure of a single phase. This phase is probably the equilibrium Cu_2Y phase.

5. Melt-spun Cu–51.1 wt % Y alloy whiskers consisted of an amorphous matrix and precipitates of an equilibrium phase, orthorhombic Cu_2Y.

Acknowledgement

References

1. K. JANSSON and M. NYGREN, *J. Less-Common Met.* **128** (1987) 319.
2. M. MARET, P. CHIEUX, P. HICTER, M. ATZMON and W. L. JOHNSON, in "Rapidly Quenched Metals V", Proceedings of 5th International Conference on Rapidly Quenched Metals (RQ5), edited by S. Steeb and H. Warlimont, Wurzburg, 1984 (Elsevier, Amsterdam, 1985) p. 521.
3. A. M. FLANK, D. RAOUX, A. NANDON and J. F. SADOC, *J. Non-Cryst. Solids* **61–62** (1984) 445.
4. J. M. FRIGERIO, M. MARTIN, J. RIVORY and T.M. DUC, "Rapidly Quenched Metals V", Proceedings of 5th International Conference on Rapidly Quenched Metals (RQ5), edited by S. Steeb and H. Warlimont, Wurzburg, 1984 (Elsevier, Amsterdam, 1985) p. 1003.
5. W. C. CHEN and A. ATRENS, in "Step into 90's", Transaction of the First Joint Conference on Corrosion, Finishing and Materials, Gold Coast, Australia, 1989, edited by A. Atrens, M. Pennisi and P. Schweinsberg (Australian Corrosion Association, Australian Institute of Metal Finishing and Institute of Metals and Materials Australia, Parkville, Vic., 1989) p. 829.
6. X. ZHANG and A. ATRENS, *Int. J. Rapid Solidifn.* 7 (2) (1992) 83.
7. X. ZHANG, P. M. KELLY and A. ATRENS, *Acta Metall. Mater.* **41** (10) (1993) 2877.
8. J. REEVE, G. P. GREGAN and H. A. DAVIES, in "Rapidly Quenched Metals V", Proceedings of 5th International Conference on Rapidly Quenched Metals (RQ5), edited by S. Steeb and H. Warlimont, Wurzburg, 1984 (Elsevier, Amsterdam, 1985). p. 203.
9. E. KNELLER, Y. KHAN and U. GÖRRES, *Z. Metallkde* 77 (1986) 152.
10. R. C. BUDHANI, T. C. GOEL and K. L. CHOPRA, in "Rapidly Quenched Metals IV", Proceedings of 4th International Conference on Rapidly Quenched Metals (RQ4), Sendai, Japan, 1981, edited by T. Masumoto and K. Suzuki (Japan Institute of Metals, 1982) p. 615.